

Superior and Anterior Inferior Cerebellar Arteries and Their Relationship with Cerebello-pontine Angle Cranial Nerves Revisited in the Light of Cranial Cephalometric Indexes: A Cadaveric Study

Kranial Sefalometrik Değerlendirme ile Süperior ve Anterior İnfierior Serebellar Arterlerin Serebellopontin Açığı ve Kranial Sinirler ile Olan İlişkisinin Değerlendirilmesi: Kadavra Çalışması

Zohreh HABIBI, Ali Tayebi MEYBODI, Farid MALEKI, Seyed Ali Fakhr TABATABAI

Imam Khomeini Hospital, Department of Neurosurgery, Tehran, Islamic Republic of Iran

Correspondence address: Ali Tayebi MEYBODI / E-mail: tayebi_a77@yahoo.com

ABSTRACT

AIM: The aim was to clarify the anatomical features of the superior and anterior inferior cerebellar arteries in relation to the trigeminal nerve and acoustic-facial complex and to the bony structures of the skull in a sample of male Iranian cadavers.

MATERIAL and METHODS: Bilateral dissections, calvariectomy, and brain evacuation were performed on 31 adult human fresh brains and skull bases to assess the neurovascular associations, and skull base morphometry. Equations were defined to estimate posterior fossa volume and the relationships between bony and neurovascular elements.

RESULTS: Eight SCAs were duplicated from origin. There were 9 cases of SCA-trigeminal contacts, which were at the root entry zone in 7. Mean distance from the origin of AICA to the vertebrobasilar junction was 11.80 mm, while 79% of AICAs originated from the lower half of the BA. This was significantly associated with "posterior fossa funneling" and "basilar narrowing" indexes. In most cases AICA crossed the acoustic-facial complex and coursed between neural bundles (48.3%). The AICA reached or entered the internal acoustic canal in 22.6% of cases and was medial to porous in 77.4%.

CONCLUSION: We documented anatomical variations of the superior and anterior inferior cerebellar arteries along with some cephalometric equations with relevant neurovascular anatomy in Iranian cadavers.

KEYWORDS: Anatomy, Acoustic-facial complex, Anterior inferior cerebellar artery, Basilar artery, Superior cerebellar artery, Trigeminal nerve, Cadaveric study

ÖZ

AMAÇ: İran kökenli erkek kadavralarda, süperior ve anterior inferior serebellar arterlerin trigeminal sinir, akustik-fasial kompleks ve kemik yapılar ile olan ilişkilerinin belirlenmesi.

YÖNTEM ve GEREÇLER: Kafatası kubbesi çıkarılan 31 kadavrada çalışma yapıldı. Serebrum dokusu tamamen çıkarıldıktan sonra posterior fossa yapılarının nörovasküler ilişkileri kemik yapıları ile birlikte morfometrik açıdan değerlendirildi. Posterior fossanın hacmi ile kemik ve vasküler yapılar arasındaki morfometrik ilişkiye göre eşitlikler belirlendi.

BULGULAR: Süperior serebellar arter 8 kadavrada başlangıçtan itibaren çift olarak izlendi. Süperior serebellar arter ve trigeminal sinir arasında 9 kadavrada temas olduğu görüldü, bunlardan ikisinde olan temas trigeminal sinir giriş noktasındaydı. Anterior inferior serebellar arter ile vertebrobasiler bileşke arasındaki ortalama uzaklık 11,80 mm bulundu ve anterior inferior serebellar arter %79 olguda basiller arterin alt yarısından çıkıyordu. Posterior fossa hunileşmesi (Funneling) ve basiller daralma indeksi ile anterior inferior serebellar arterin basiller arterin alt yarısından çıkması arasında ilişki bulundu. Olguların çoğunda anterior inferior serebellar arter akustik fasial kompleks ile çaprazlaşıyor ve nöral lifler arasında seyrediyordu (%48,3). Anterior inferior serebellar arter internal akustik kanalın ya içerisine kadar ilerliyor (%22,6) ya da kanalın medial yüzeyine temas ediyordu (% 77.4).

SONUÇ: İran kökenli insanlarda süperior serebellar arterin ve anterior inferior serebellar arterin varyasyonları, nörovasküler ilişkileri yanı sıra bu ilişkilere dayanarak bazı sefalometrik eşitlikler de oluşturuldu.

ANAHTAR SÖZCÜKLER: Anatomi, Akustik-fasial kompleks, Anterior inferior serebellar arter, Basiller arter, Süperior serebellar arter, Trigeminal sinir, Kadavra çalışması

INTRODUCTION

The trigeminal nerve and acoustic-facial complex are involved in various pathologies of the CP angle. Their intimate relationship with the SCA and AICA respectively, increases the hazards of surgical approach to this region. Hence, a comprehensive knowledge of neurovascular variations is crucial to deal with the various pathologies in this region safely and confidentially (15, 16, 23). Various anatomical, clinical and radiological studies of cerebello-pontine angle, with the main focus being on cranial nerves and vasculature, have been designed to meet this purpose (1, 2, 4, 6, 7, 22).

To the best of our knowledge, the neurovascular relations of the trigeminal nerve and acoustic-facial complex, as well as their relationships to the bony structures of the skull, have not been previously studied in Iranian population. The aim of the present study is to clarify this anatomy in a cadaveric study on a sample of Iranian population. As many other conditions, nationality or race may influence the anatomy.

MATERIAL and METHODS

Gross anatomy of posterior fossa neurovascular compositions and skull base bony indexes were recorded in 31 fresh male human cadaveric brains. Death was not caused by traumatic brain injury. All pathologic conditions that could influence the normal anatomy of the posterior fossa and/or the whole brain were excluded (e.g., tumor, arteriovenous malformation, infection). Dissections were performed within 24 hours postmortem. The age of cadavers at the time of death ranged from 20 to 78, with the mean being 45.5 years. Female cadavers were not included because of cultural and legal limitations.

Bilateral dissections were performed on CP angles of the brains. The dissection process is defined below:

"A bicoronal scalp incision was made and a calvariectomy was performed from just above the nasion to theinion. An axial cut through the hemispheres caused a small portion of the central core (diencephalon) and lower temporal lobes to remain attached to the brain stem. At the next step, the central core was detached and discarded, leaving the circle of Willis and the lowest part of the diencephalon attached to the brainstem. Next, both optic nerves and carotid arteries were cut such that the chiasm and the attached part of the upper mesencephalon could be reflected backward to expose the pre-pontine area. The tentorium was cut bilaterally parallel to superior petrosal sinus and reflected backwards. This maneuver exposed the cerebello-pontine angle bilaterally from above. The scope of the posterior fossa vasculature specifically SCA and AICA branches, the relations of the cranial nerves III-V to the SCA, and the associations between acoustic-facial complex and the AICA were examined with the brainstem in situ, with the aid of surgical loupe, which was also used in the following steps of dissection and measurements. The SCA dimensions and neural relations were recorded first, before bilateral trigeminal nerves section to facilitate exposing the AICAs, proximal basilar

artery, and acousticofacial complex. Measurements of the outer diameters of the basilar arteries (BA), SCA, AICA, and their branches were performed using Collis caliper by one examiner (A.T.M.) and were checked by the other one (Z.H.). The lengths of the vessels' segments were measured from the midpoint of bifurcations and/or arterial take off place to the midpoint of the next bifurcation and/or take off place by the former examiner and checked by the latter one. The distances between two adjacent structures were recorded by measuring the perpendicular span from the mid-point of one to another; for instance, a line drawn from the midpoint of the root entry zone of the nerve VI to a plumb midline of BA represented Basilar-Abducens distance. The variables listed in Table I were studied. Next, the brainstem and cerebellum were removed by a sharp cut through cervicomedullary junction. The osseous morphometric variables were measured after posterior fossa neurovascular relationships were examined on the extracted brainstem (Table I and II)."

The following variables were also measured on the bony skull base (Table III):

1. Inter-pterional distance: the distance between the most lateral parts of the sphenoid ridges where they reach the parietal bone (A)
2. Endinion-sella: the length of a straight line drawn from the internal occipital protuberance (IPO) to the middle point of the dorsum sellae (B)
3. Endinion-nasion: the length of a straight line from the IOP to the most anterior point in the middle of the anterior cranial fossa (corresponding to the external point "nasion") (C)
4. Petrous length: the length of petrous ridge from posterior clinoid process to the most posterolateral point on the petrous ridge (roughly the point where the superior petrosal sinus meets the transverse sinus) (D)
5. Petrous-trigeminal distance: distance between the most postero-lateral point of petrous ridge to the point where the trigeminal nerve root passes on the petrous ridge (E)
6. Inter-petrosal distance: the distance between the most posterolateral points of the two petrous ridges corresponding to the highest level of sigmoid sinus (F).
7. Anteroposterior dimension of the foramen magnum in the midline (G)
8. Transverse diameter of the foramen magnum: the greatest transverse diameter of the foramen magnum (H)
9. Height of posterior fossa: the length of a line passing perpendicularly from the foramen magnum plane ending at the level of endinion-sella line (I)

Descriptive statistics was applied to declare numerical results as mean, maximum, minimum, and standard deviations. Statistical Package for Social Science (SPSS) version 18 was employed for statistical analysis. Regression Analysis was used to examine correlation between non-parametric variables. Student t-test was used to compare means between parametric variables. p value of less than 0.05 was considered to affirm significant associations.

RESULTS

Summary of results are depicted in Tables I-IV.

1. Vascular Relationships

1.1 Basilar Artery

The basilar artery diameter was measured at two points: proximal part (just distal to the junction of the vertebral arteries) and distal part (just proximal to the origin of PCAs). Mean proximal diameter was 4.99 mm (2.80-7.70) and mean distal diameter was 3.90 (2.10-5.00).

1.1-1 Basilar Deviation

To quantify the deviation of the BA from origin to its bifurcation alongside the brainstem in coronal plane (according to its relation to the REZ of abducens nerves), "basilar deviation index" was calculated as:

$$BasDev = \frac{LBA - RBA}{LBA + RBA} \quad (1)$$

LBA and RBA stand for the distances from the midpoints of the BA to the root entry zones of the left and right abducens nerves, respectively. When the value is 0, it means that the basilar artery courses straightly, and when it is -1 it shows complete left deviation, while when it is +1 it means that the basilar artery touches the right 6th nerve REZ (implying right sided curve along the brainstem). Basilar deviation to left or right was almost equally distributed. Three cases showed complete deviation of basilar artery such that it touched the REZ of 6th nerve. The distance between the basilar artery and the REZ of AFB was also measured in 62 CP angles, with the mean value being 14.12 mm (1.40-23.50mm). Basilar artery

Table I: The Descriptive Neurovascular Variables are Tabulated as Basilar, Sca, and Aica Categories

Parameter	Mean (mm)	Standard deviation	Minimum (mm)	Maximum (mm)
BA				
Basilar length	29.6723	5.56177	22.2	46.00
Proximal basilar diameter	4.9890	1.13552	2.80	7.70
Distal basilar diameter	3.8987	0.74365	2.10	5.00
Left bas to abducens distance	7.2445	3.28017	0.00	16.55
Right bas to abducens distance	7.4639	2.61815	0.00	13.00
Left bas to AFB distance	13.8419	4.64477	1.40	21.10
Right bas to AFB distance	14.4045	5.36047	0.00	23.50
SCA				
Left SCA diameter	1.6645	0.41497	0.00	2.20
Right SCA diameter	1.6368	0.50543	0.00	2.40
Left rostral SCA trunk diameter	1.3026	0.36634	0.60	2.00
Right rostral SCA trunk diameter	1.3938	0.27238	1.00	2.00
Left caudal SCA trunk diameter	1.3636	0.38962	0.70	2.40
Right caudal SCA trunk diameter	1.3607	0.35272	0.80	2.20
Left SCA origin to bifurcation	14.9610	10.031	0.00	35.10
Right SCA origin to bifurcation	14.7742	10.750	0.00	34.00
AICA				
Left AICA diameter	1.3475	0.78560	0.3	4.80
Right AICA diameter	1.3907	.46269	.28	2.45
Left basilar origin to AICA	12.0116	5.66920	3.20	24.76
Right basilar origin to AICA	11.6100	4.57699	0.50	22.50
Left AICA origin to bifurcation	14.9938	10.636	0.00	34.00
Right AICA origin to bifurcation	14.6000	6.08714	8.70	24.90
Left AICA origin to AFB REZ	15.8797	2.50589	10.60	21.70
Right AICA origin to AFB REZ	16.1180	3.59472	11.30	29.50

Table II: Neurovascular Relationships for SCA-Trigeminal Complex and AICA-Acousticofacial Complex

Parameter	Mean (mm)	Standard deviation	Minimum (mm)	Maximum (mm)
SCA-Trigeminal*				
Left SCA contact distance from artery origin	17.84	3.52	14.00	23.20
Right SCA contact distance from artery origin	23.42	2.24	20.40	25.80
Left SCA diameter at the contact point	1.10	0.12	0.90	1.20
Right SCA diameter at the contact point	1.31	0.40	0.95	1.80
AICA-Acousticofacial†				
Left AFB cross to AICA origin	17.33	2.81	0.00	22.00
Right AFB cross to AICA origin	18.35	4.15	9.50	28.30
Left AFB cross to anterior IAC distance	8.33	4.05	2.20	23.10
Right AFB cross to anterior IAC distance	8.43	3.73	0.00	16.20

*There were 9 cases of SCA-5th nerve contact.

†There were 57 cases of AICA-7,8th nerve complex crossing.

Table III: Morphometric Bony Skull Base Parameters

Parameter	Mean (mm)	Standard deviation	Minimum (mm)	Maximum (mm)
Endinion to sella distance	87.0748	10.048	69.00	107.30
Nasion to endinion distance	147.67	8.78257	133.00	168.00
Interpterial distance	107.58	8.46976	88.80	119.00
Interpetrosal distance	121.21	13.030	95.38	149.07
Left petrous length	72.1355	5.97916	59.00	84.40
Right petrous length	70.7071	6.25413	57.90	82.00
Left petrous-trigeminal porus distance	53.8387	6.12066	38.00	66.60
Right petrous-trigeminal porus distance	52.4516	5.96898	37.00	65.00
Height of posterior fossa	60.2016	5.38894	49.09	72.47
Antroposterior diameter of foramen magnum	27.2581	5.29558	14.50	38.00
Transverse diameter of foramen magnum	27.9258	3.47371	17.30	34.00

length ranged from 22.20 mm to 46.00 mm with a mean of 29.67 mm.

1.1-2 Basilar Narrowing

If the basilar artery is traced from its origin to bifurcation, the difference between proximal and distal diameters is a crude index of arterial narrowing; translating this concept to mathematical language, one can define Basilar Narrowing (BN) as follows:

$$BN = \frac{D_1 - D_2}{D_1} \quad (2)$$

Where D1 is the diameter of proximal part of the basilar artery, and D2 is distal basilar diameter at the level of bifurcation. In this view, if BN is 0, it means that the artery has not tapered through its course (having equal proximal and distal diameters), and a BN closer to 1 indicates the other end of the spectrum, where the distal diameter gets smaller and smaller (Figure 1A,B).

1.2 Superior cerebellar artery

In all 31 cases (62 CP angles), SCA originated from the basilar artery just proximal to the origin of posterior cerebellar artery. The SCA diameter varied from hypoplastic (< 1 mm) to 2.40 mm (mean 1.65 mm). Duplication was seen in 8 SCAs and in one case the vessel was triplicated. In all cases, the SCA showed a modest caudal loop approximating the REZ of trigeminal nerve; in 9 cases this caudal loop reached a contact point on the origin of cranial nerve V (Figure 2). The mean length of SCA up to bifurcation point was 14.96 mm in left and 14.77 mm in right (0.00 mm – 35.10 mm). Two contacts were by the main SCA trunk and the remaining 7 contacts were by the caudal trunk of SCA. Fifty two cases showed a close contact between the third cranial nerve and SCA.

1.2-1 SCA bifurcation

Eight SCAs were duplicated and we found one triplicated SCA. The rostral and caudal trunks were almost equal in diameter (mean of rostral trunk diameter 1.35 mm, mean caudal trunk

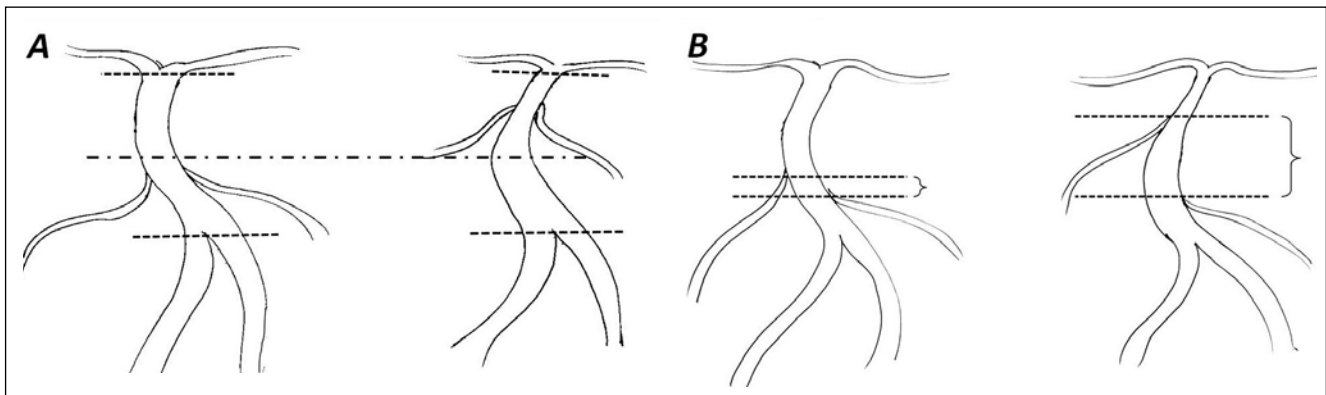


Figure 1: Basilar narrowing. **A)** The mean of basilar narrowing index was higher in those with higher AICA origin. **B)** Basilar narrowing was more prominent in cases with the higher AICA discrepancy index.

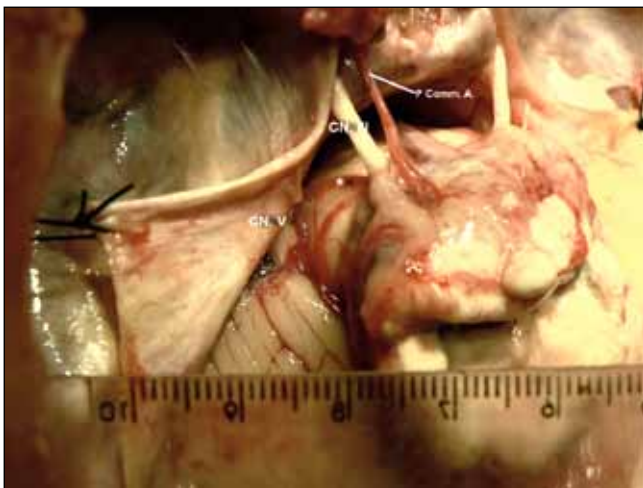


Figure 2: Cadaveric dissection of the brain showing the caudal trunk of the left superior cerebellar artery (*) traveling a long course to touch the superior pole of the trigeminal nerve root (CN. V). Tentorium is incised and sutured anteriorly to expose the pre-pontine cistern. **CN.**, cranial nerve, **P Comm A.**, posterior communicating artery.

diameter 1.36 mm) (Table I). The rostral trunk was hypoplastic in 7 cases (less than 1 mm diameter), and the caudal trunk was hypoplastic in 15 cases.

1.3 Anterior Inferior Cerebellar Artery (AICA)

The mean AICA diameter was 1.32 mm (0.30 to 2.45 mm), with 14 cases being categorized as hypoplastic (less than 1 mm). There was one duplicated AICA in this series. In all CP angles studied, the AICA originated from the basilar artery, and we found 5 cases of AICA-PICA variants originating from the basilar or ipsilateral vertebral artery. In 13 cases (20.9%) AICA originated from the upper half of the basilar artery, but in most cases it came from the lower half of the artery. The position of AICA origin in the course of the basilar artery was significantly correlated with posterior fossa funneling (defined later); so that the average PF funneling was greater in group with AICA origin on the upper half of the basilar artery

course (p value < 0.05) (Figure 3, Table IV). Basilar narrowing was significantly related to AICA origin while the mean of basilar narrowing index was higher in cases of upper AICA origin (p value < 0.05) (Figure 1A, Table IV). The AICA or its main trunks crossed the acoustic-facial bundle in 57 cases (91.9%). This crossing happened at some distance from the AFB REZ and none was in touch with the point of entrance of the AFB to the brainstem.

1.3-1 AICA perimeatal segments

The AICA meatus related parts - namely pre-meatal, meatal, and post-meatal segments - are those that course in the vicinity of the porus of the acoustic-facial bundle. Each segment consists of one or two trunks according to the position of the artery bifurcation related to the meatus, (e.g. whether bifurcation taking place after or before the acoustic-facial porus). In this series of 62 CP angles there were 63 pre-meatal, 65 meatal, and 71 post-meatal segments.

1.3-2 AICA discrepancy

The origin of the two AICAs is not always at the identical level. The relative distance between the origins of the two AICAs can be defined as "AICA discrepancy" which can be calculated as follow:

$$AICA\ discrepancy = \frac{|left\ AICA\ origin - Rt\ AICA\ origin|}{basilar\ length} \quad (3)$$

Where left AICA origin is the distance between the vertebrobasilar junction to the left AICA take off point, and right AICA origin is defined in similar way as well.

In this series, the mean AICA discrepancy was 0.097 (ranging 225 from 0 to 0.27). AICA discrepancy was significantly associated (p value = 0.003) with the basilar narrowing [AICA discrepancy = 0.265 * (basilar narrowing) + 0.44]. Indeed, in cases with more difference in the AICAs take off points (manifested as the higher AICA discrepancy index), basilar narrowing was more prominent. On the other hand, in those with lower difference in the proximal and distal BA diameters indicating as lower basilar narrowing, the AICA discrepancy

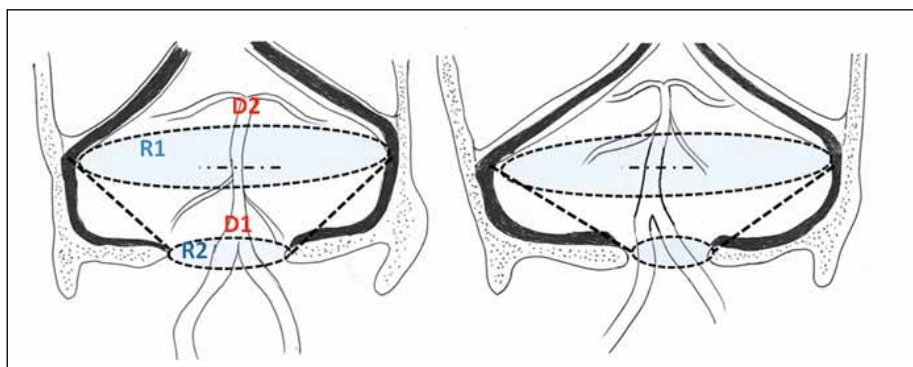


Figure 3: Posterior fossa funneling. The funneling index was greater in the group with AICA origin on the upper half of the basilar artery than that of lower AICA origin group. Compare two sides with different funneling ratios and difference in AICA origin. Initials in the figure are according to equations 2 and 10.

Table IV: Some of Significant Correlations^a

Statistically Dependent Variables	Independent Variables
Basilar Deviation ^b	SCA-Trigeminal Contact, Trigeminal Depth ^c
Basilar Narrowing ^d	AICA Origin, AICA discrepancy
PFV/CrV ^e	Cranial Funneling
Cranial Elongation ^f	Cranial Volume ^g , Posterior fossa volume ^h

^a *p* value < 0.05 was considered as significant.

^b As defined in equation 1, a more basilar deviation correlated with a more probability of SCA-trigeminal contact.

^c As defined in equation 4, a more basilar deviation correlated with a more medially located insertion point of the trigeminal nerve root on the petrous ridge, hence a "deeper" trigeminal nerve.

^d As defined in equation 2, the higher magnitude of basilar artery narrowing through its course correlates with a higher origin of AICA on the parent artery; it also correlated with a higher AICA discrepancy index as defined in equation 3.

^e Equation 11. When the posterior fossa comprises a higher proportion of the total cranial volume, the funneling ratio (equation 10) is higher.

^f Equation 12.

^g Equation 13.

^h Equation 14.

ratio was lower (Figure 1B). Table IV summarizes some significant correlations found between the measured and defined variables in this study.

2. Neural Relationships

2.1 The Oculomotor nerve

In 37 cases there was a superior-inferior contact between the oculomotor nerve and the proximal part of the SCA. There was no contact point in 10 cases, and the relationship was medial-lateral and infero-lateral in 9 and 6 cases, respectively. The length of vessel between its origin and its point of contact with the oculomotor nerve averages 5.00 mm (range, 2.00–8.00 mm). In 18 cases the rostral trunk of SCA was related to the oculomotor nerve (post-bifurcation contact).

2.2 The Trochlear Nerve

The relationship between the 4th CN and the SCA (or its branches) adjacent to the free edge of tentorium was found to be as follows: (1) medial-lateral, (37 cases, 59.7%), (2) superior-inferior (16 cases, 25.8%), (3) no contact (9 cases, 14.5%).

2.3 The Trigeminal Nerve

There were 9 contacts between the SCA and trigeminal nerves at its origin. Five contacts were at the superomedial pole of the trigeminal root and the remaining 4 were at the superior pole of the trigeminal root. The mean distance between

the origin of the artery to the contact point with trigeminal nerve was 20.32 mm (14.00 – 25.80 mm). This contact point was at the very origin of the trigeminal root entry zone from the brainstem in seven cases and in the remaining two, it was 4.00 and 5.00 mm from the nerve origin. The mean diameter of SCA (or its branches) at the contact point was 1.20 mm (range, 0.90-1.80 mm). Mean basilar deviation in cases that the nerve touches SCA (or its branches) is 0.4 compared to basilar deviation in cases that the nerve does not touch the SCA (0.05); independent t-test (*p* value = 0.025) shows the difference to be statistically significant (Figure 4A,B, Table IV).

2.3-1 Trigeminal Depth

The insertion point of trigeminal nerve on the petrous ridge is not the same in different calvaria. The location of this insertion point could be defined as "trigeminal depth (TrgD)" on the petrous ridge as follows:

$$\text{TrgD} = \frac{E}{D} \quad (4)$$

Where E is petrous-trigeminal length and D indicates petrous length in Figure 1. The trigeminal depth was significantly correlated (*p* value < 0.001) with the basilar deviation index as follows:

$$\text{Basilar deviation} = 1.793 * (\text{trigeminal 267 depth}) - 1.082 \quad (5)$$

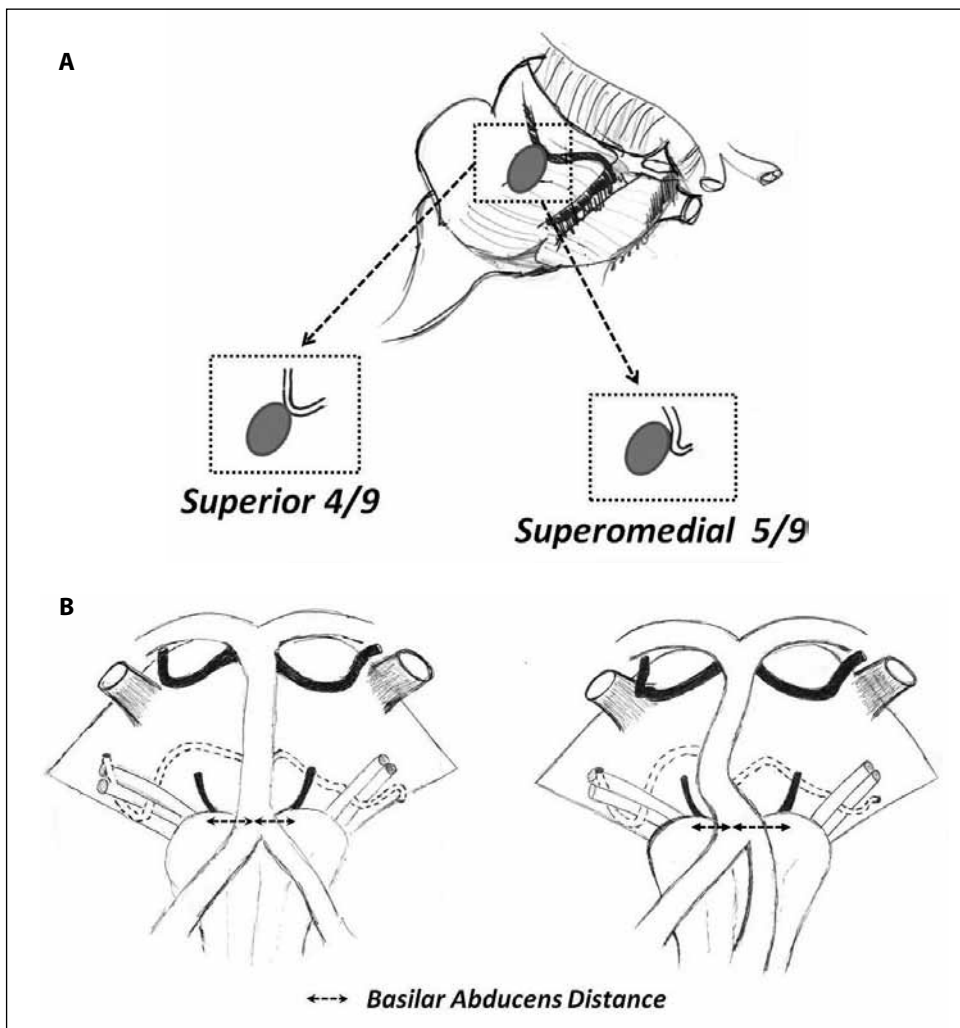


Figure 4: A) Distributive diagram of two contact variations between the SCA caudal loop and the trigeminal nerve root. **B)** The more basilar deviation, the higher probability of SCA-trigeminal contact.

2.4 The Abducens Nerve

The mean distance of the basilar artery to the abducens REZ was 7.35 mm. the basilar abducens distance was used to calculate basilar deviation as mentioned above (Figure 4A,B).

2.5 The Acoustic-facial complex

The AICA or its main trunks crossed the acoustic-facial bundle in 57 cases (91.9%). This cross was always at some distance from the entry zone of AFB to the brainstem. The average distance from the AICA origin to AFB cross was 17.84 mm, ranging from 0.00 (cross at the site of AICA origin) to 28.30 mm. The distance between the cross to the anterior aspect of internal auditory canal (IAC) was 8.38 mm in average (0 – 23.10 mm). In 5 cases there was no virtual distance between the AICA-AFB cross and IAC; indeed, the cross had taken place just at the site of the IAC.

Before reaching the porus, the AICA coursed in different ways in relation to the neural fibers of acoustic-facial complex, so that a majority of 48.3 % (30 cases) passed between the fibers, followed by 23 cases of ventral and 6 cases of dorsal course in relation to the neural bundles. In 3 cases (4.8%) the artery

passed a pathway below the AFB in a parallel course with the flocculonodular lobe of the cerebellum (Figure 5A).

At the site of the porus, the AICA did not reach the porus in 48 CP 286 angles (looped medial to the IAC) (77.4%). In 12 cases the artery or its main trunks had entered the canal, and in 2 cases it had only touched the porus without entering to the canal (Figure 5B).

3. The morphometric indexes

The following indexes and ratios were described to hypothesize some relationships of the morphometrically associated structures and spaces:

3.1 Cranial Volume

The cranium could be considered as an irregular sphere; hence its radius can be the length of petrous ridge. In this manner, the volume of this sphere will be proportional to the third power of the sphere radius (petrous length) such that:

$$CrV \propto \pi PL_3 \quad (6)$$

Where CrV is the cranial volume and PL indicates the average of the left and right petrous lengths in each cranium.

In this series, the calculated value was found to be between 628000 mm³ and 1764680 mm³ (mean 1166790 mm³). According to the equation above, this calculated value could represent an estimate of the cranial volume.

3.2 Posterior fossa volume

If one considers the posterior fossa as an incomplete cone (Figure 305 7), with the greater base being a virtual plane passing through the petrous ridges and the endinion, such that it is parallel to the virtual plane passing through the foramen magnum which is the lesser base, the volume could be computed having the height of this incomplete cone:

$$PFV = \frac{H+H'}{3} \pi R_1^2 - \frac{H'}{3} \pi R_2^2 \quad (7)$$

$$H' = \frac{R_2 H}{R_1 - R_2} \quad (8)$$

Where PFV shows posterior fossa volume, H stands for the measured height of the partial cone, and R1 and R2 are the radii of the greater and lesser bases, respectively. The average value of inter-petrosal and endinion-sella distance was considered as the greater base diameter, and the average of the anterior-posterior and lateral diameters of foramen magnum was used as the lesser base diameter. H' is the height of the small complete cone based at foramen magnum plane (calculated through equation (8) based on Thales' theorem), bearing in mind that partial cone is a volume forms by subtraction of two complete virtual cones (Figure 6).

In 31 craniums examined, the approximated posterior fossa volume was 126000 to 343000 mm³ (mean 231470 mm³) based on the equations above (6 and 7). The accuracy of the formula was tested in 10 skulls by water filling method, which found the calculated value to be roughly similar to the measured volume (with at most 4 to 10 cm³ differences).

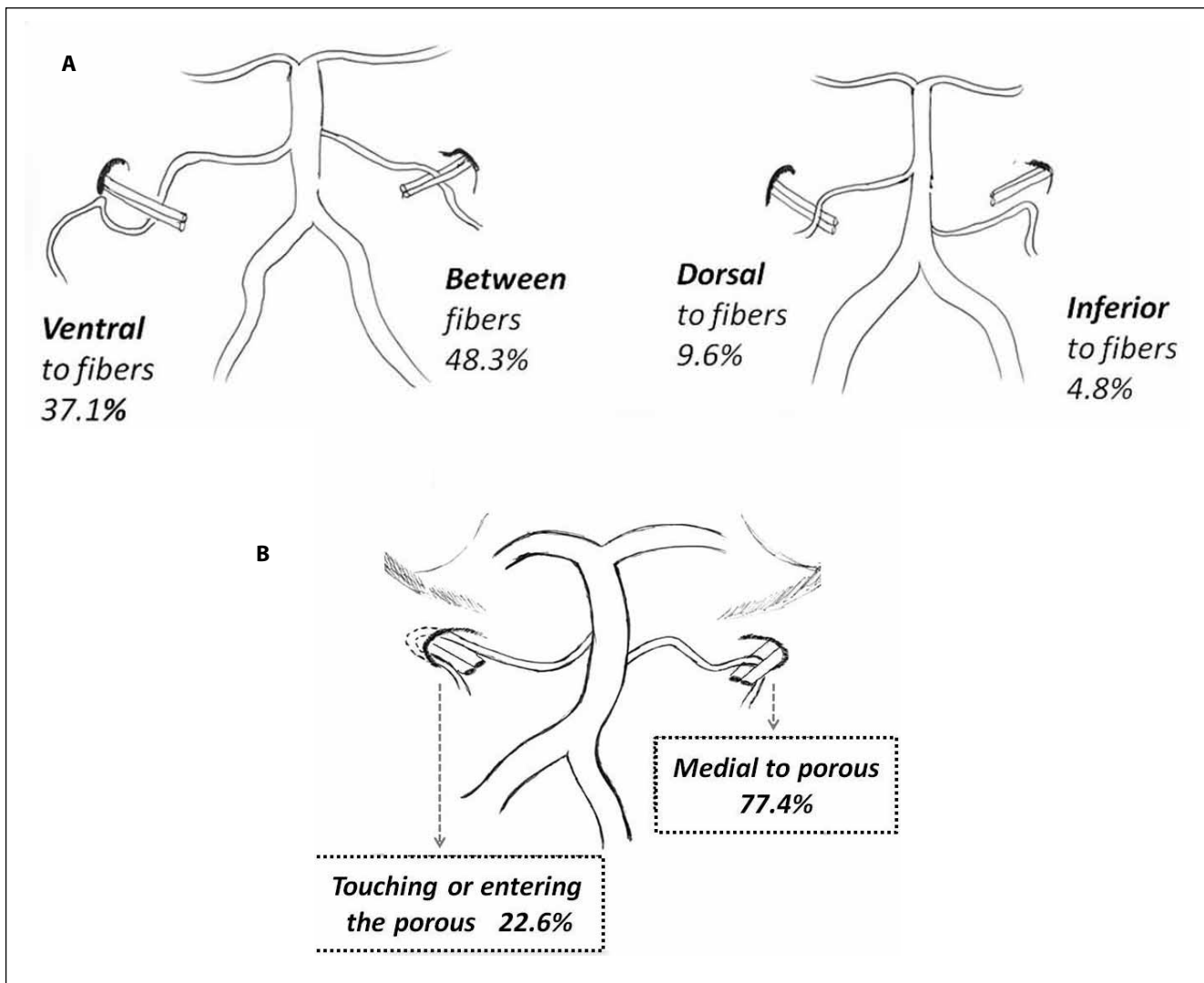


Figure 5: A) Different anatomical variations of AICA-AFB association. B) Frequency of two main type of AICA-IC relationship in the current study.

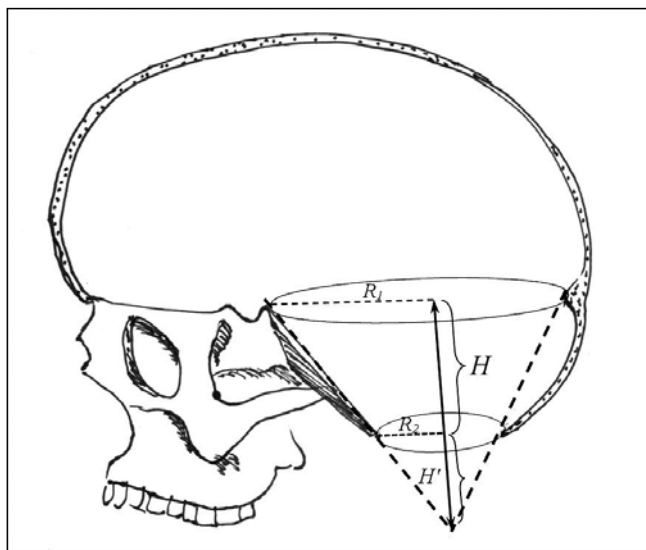


Figure 6: Geometric illustration to describe the mathematical approach to calculate the posterior fossa volume (see equations 7 & 8 in text).

The cranial volume estimate was significantly (p value < 0.001) correlated to calculated posterior fossa volume:

$$PFV = 0.484 * (CrV) + 51450.746 \quad (9)$$

3.3 Posterior fossa funneling

The more the difference between R_1 and R_2 (Figure 6), then we will have a posterior fossa more resembling a funnel (i.e. it is closer to a complete cone). Therefore, a funneling ratio

(FR) could be defined as follows:

$$FR = \frac{R_1 - R_2}{R_1} \quad (10)$$

Funneling ratio in our study ranged from -0.12 to 0.54, with a mean of 0.26.

The ratio of calculated posterior fossa volume to the estimated cranial volume (PFV/CrV) was significantly correlated (p value < 0.001) to the funneling ratio of the posterior fossa as follows:

$$PFV / CrV = 0.943 * (FR) + 0.38 \quad (11)$$

3.4 Cranial Elongation

Cranial elongation shows how much the axial plane of the cranium is circular or elliptical.

This could be calculated as the ratio of the greater and lesser diameters of the ovoid cranium in axial section, as follows:

$$CrE = \frac{C}{\frac{A+F}{2}} \quad (12)$$

Where according to Figure 1, C indicates nasion-endinion distance (greater diameter), A is inter-pterional distance, and F is the inter-petrosal distance. The $(A+F)/2$ is an average index of the lesser diameter.

The elongation ratio ranged from 1.09 to 1.59 in our 31 examined craniums (mean 1.29).

Cranial elongation was significantly related to both the crude estimate of cranial volume

(3rd power of petrosal length multiplied by π) and calculated posterior fossa volume (p value < 0.001).

$$CrV = -382929.554 * (CrE) + 869192.527 \quad (13)$$

$$PFV = -220390.017 * (CrE) + 517856.898 \quad (14)$$

DISCUSSION

Practically, anatomical dissections in cadavers cannot fully simulate the in vivo circumstances encountered by the surgeon while operating on the posterior fossa (6).

Methods such as fixation and perfusion have been tried to overcome this problem (3, 10, 12); however, there have also been drawbacks with them (11) and neurovascular relationships may still not reflect those that would be found at operation if perfusion and subsequent fixation are done at non-physiological pressures, or in a different position from that employed at surgery (6). Some series have used fresh brains without fixation or perfusion as we have done (14, 22); although it seems clear that in such a design one could not fully rely on the measurements (especially vessel diameters) and the neurovascular relationships.

In this series, the authors studied the neurovascular contents of CP angels, as well as some morphometric indexes in 31 fresh cadaveric brains. Limitation of examination of female cadavers in Iran is a drawback of our study as it could not represent the general population of course.

1. Basilar Artery

1.1. Basilar Artery Course

In this series, none of the basilar arteries examined ran a completely midline straight course, except one case with the basilar deviation ratio of zero. However, with the assumption that the basilar deviation ratio of less than 0.1 is an indicator of a roughly straight course, 45% of the arteries were straight. These results are comparable to that of Yasargil's series representing only 25% of all cases to be in thorough straight course (24). On the contrary, Pai et al found a majority of 74% in midline straight direction (16).

Since neither of the mentioned previous studies used a quantitative measure, comparison between our results and the other two will not yield a meaningful result.

1.2. Basilar Artery Narrowing

The basilar artery narrows during its course toward the inter-peduncular fossa (equation 2). The extent of narrowing seemed to be related significantly to the following measured variables: (1) AICA discrepancy (p value = 0.003), (2) AICA origin (p value = 0.033), and (3) SCA/AICA diameter (p value = 0.001); i.e., in cases with more tapering BA, the proportion

of SCA diameter to AICA was higher. Basilar narrowing was higher in those with upper AICA origin, and the discrepancy between two AICAs take off points was more in those with higher BA narrowing value (Table IV, Figure 1).

2. Superior cerebellar Artery

The superior cerebellar artery usually arises from the terminal part of basilar artery just before its bifurcation and turns around the brainstem to reach the cerebello-mesencephalic fissure. It may be duplicated from its origin (Figure 7). In this series, we found 8 cases to be duplicated (12.9%); roughly similar to Pai and Rhoton reports of 12% (6/50) and 14% (7/50) rate of SCA duplication (16, 17).

The SCA diameter was averagely 1.65 mm in our 62 cases, while Pai et al reported mean left and right SCA diameter to be 1.6mm and 1.4mm, respectively (16).

The distance from origin to bifurcation of the SCA ranged from 0.00 – 35.10 mm, compared to a previous study that reported a range of 0.6-43 mm (mean 19 mm) (17).

Fifty-two cases examined showed a contact point between the SCA and the oculomotor nerve, from which 37 (59.6%) contact points were in superoinferior direction. The results are comparable to those of Rhoton et al (contact rate of 66%, mostly superior-inferior) (17).

2.1. Trigeminal Nerve Relationships

There were 9 contacts (14.5%) between the trigeminal nerve at its origin and the SCA.

Rhoton et al reported a contact rate of 435 12% between the trigeminal root and the SCA or its branches (17). The mean diameter of SCA (or its branches) at the contact point was 1.20 mm (range, 0.90-1.80 mm) in our study and 1-2 mm in Rhoton series (17). If the basilar artery is more deviated from the midline, the probability of SCA contact with the trigeminal nerve root is higher (p value = 0.025). Side of basilar deviation does not influence the side of nerve-artery contact. In five cases of nerve-artery contacts, the main trunk of SCA was in contact with the nerve and in the remainder it was by the caudal trunk of SCA. Rusu et al has mentioned 35% contact by the main trunk and the rest by the caudal (lateral) SCA trunk (18).

3. Anterior Inferior Cerebellar Artery

Anterior inferior cerebellar artery supplies the petrosal surface of the cerebellum and important elements in CP cistern (8). It has a variable origin and course. In this series, most cases originated from the lower half of basilar artery (mean distance of AICA origin from the basilar artery origin was 12.10 mm on left and 11.61 mm on right). Concordantly, in Yasargil's series 84% of AICAs branched from the lower third of BA (24). On the contrary, Pai et al state that the most common origin of the AICA (62%) is the upper half of the basilar trunk (16).

We found one duplicated AICA, while others have found a 20-26% rate of duplication (16, 17, 24).



Figure 7: Bilateral duplicated superior cerebellar arteries, anterior view. Both posterior cerebellar arteries are sutured with black thread. **Bas.**, basilar artery, **Cerebel.**, cerebellum, **CN.**, cranial nerve, **ON.**, optic nerve, **Pit. Fos.**, pituitary fossa.

3.1. Acoustic-facial Complex Relationships

In all cases except the 5 AICA-PICA variants, the artery crossed the acoustic-facial bundle.

AICA usually bifurcates in the vicinity of the acoustic-facial bundle. Rhoton et al have found this bifurcation to be before the nerve-artery crossing in 66% of cases (17). In our study, the bifurcation occurred before the cross in only 24.2%. Difference in preparation technique (fresh brains vs. fixated perfused brains) might explain the discrepancy. The nerve-related segments of AICA course in or near the porus of the internal acoustic meatus. In the 50 CP angles examined by Rhoton and colleagues, there were 56 nerve-related pre-meatal segments (88% solitary), 59 meatal segments (82% solitary), and 60 post-meatal segments (80% solitary) (17). Accordingly, In 62 CP angles we studied, there were 63 pre-meatal (single in 91% of cases), 65 meatal (85% single), and 71 post-meatal segments (74% single).

The course of AICA in proportion to the acoustic-facial bundle was variable in our series, with a majority of 48.3% moving between fibers; 37.1% ventral, 9.6% dorsal, and 4.8% inferior to nerve fibers. Yurtseven et al studied 24 cadavers, and found 32% of AICAs ventral and 35% dorsal to the 7th-8th neural complex, and in 32.5% the artery passed between the fibers (25).

We localized the artery to be in medial position to the porus of IAC in 72% of cases, whereas the remainders touched or entered the meatus. In the series of Rhoton et al, AICA was located medial to the porus in about half of CP angles and looped to reach the porus or protruded into the canal in the other half (17). However, two other studies found the loop of AICA to be at the porus or within the canal in majority of cases (64% and 67%) (13, 21). This inconsistency could be due to different definitions of the position of the meatal loop of AICA regarding the porus of IAC in different studies.

Although at first glance it may be conceptualized that in cases with larger coronal diameter of posterior fossa the AICA might

enter the canal less probably, in our series the relationship of the AICA to the IAC had no significant association with the inter-petrosal diameter (p value > 0.05). Hence, it can be concluded that the course of AICA around or in the canal is dictated by the length and tortuosity of the artery itself, rather than the structural dimensions of the skull.

4. Morphometric Indexes

There have been some efforts to extract relationships between the craniometric indexes and intracranial soft tissue measures (5, 19, 20). We have also tried to find such relationships between craniometric indexes and the features of the arteries of the posterior fossa and their relationship with the neural complexes. We managed to establish mathematical equations to estimate volume of the cranial cavity and the posterior fossa volume in order to facilitate quantification of the values.

The volumetric variables such as cranial volume, cranial elongation, posterior fossa volume, and inter-petrosal distance were found to have no significant association with the neurovascular elements of cerebello-pontine cistern (p value > 0.05). However, the funneling ratio of the posterior fossa had a roughly meaningful correlation with the AICA origin upon the BA (p value = 0.05). On the other hand, some of the cephalometric indexes were found to be significantly related to each other (e.g., cranial volume and cranial elongation). In general, one can conclude that the relationships between the neurovascular components of this region should be more dependent on the courses, lengths, and diameters of such elements themselves, rather than the dimensions of the bony containers, although opposite views are existent too (9, 22).

Of course, this crude hypothesis needs to be tested with a larger sample size, and weighed against the results of volumetric and angiographic radiological evaluations.

This study had some limitations that include lack of a microscope, lack of the antemortem history of the cadavers, and exclusive examination of male cadavers. Also, some non-significant associations may have been due to relatively low sample size.

CONCLUSION

The present study, performed on 31 fresh human cadavers, describes some of the anatomic properties of the posterior fossa neurovasculature in a sample of male Iranian population. Although the method used does not fully simulate the techniques used in other studies in this field, the results seem to be in concordance with most of previous studies. Correlation of the cadaveric data with the *in vivo* and/or radiological information can lead to new concepts in the pathophysiology of cranial nerve compression syndromes.

The cephalometric indexes proposed in the current study, though being arbitrary, might be a substrate for further studies to delineate the relationship between the rigid structures of cranium and the soft tissues within.

Future studies may deal with the clinical and radiological correlates of post-mortem findings, with more sample size. Possible elucidation of genetic basis of the anatomical differences might be a prudent speculation.

DISCLOSURE

The authors report no conflict of interest concerning the materials or methods used in this study or the findings specified in this paper.

ABBREVIATIONS

- AFB** Acoustic-facial bundle
- AICA** Anterior inferior cerebellar artery
- BA** Basilar artery
- CP** Cerebello-pontine
- CrV** Cranial Volume
- IAC** Internal auditory canal
- PCA** Posterior cerebral artery
- PF** posterior fossa
- PICA** Posterior inferior cerebellar
- REZ** Root entry zone
- SCA** Superior cerebellar artery
- SPSS** Statistical Package for Social Science

REFERENCES

1. Anderson VC, Berryhill PC, Sandquist MA, Ciaverella DP, Nesbit GM, Burchiel KJ: High-resolution three-dimensional magnetic resonance angiography and three dimensional spoiled gradient-recalled imaging in the evaluation of neurovascular compression in patients with trigeminal neuralgia: A double-blind pilot study. *Neurosurgery* 58: 666-673, 2006
2. Boecher-Schwarz HG, Bruehl K, Kessel G: Sensitivity and specificity of MRA in the diagnosis of neurovascular compression in patients with trigeminal neuralgia: A correlation of MRA and surgical findings. *Neuroradiology* 40: 88-95, 1998
3. de Oliveira E, Rhoton AL Jr, Peace D: Microsurgical anatomy of the region of the foramen magnum. *Surg Neurol* 24: 293-352, 1985
4. Fukuda H, Masatsune I, Ryosuke O: Demonstration of neurovascular compression in trigeminal neuralgia and hemifacial spasm with magnetic resonance imaging: Comparison with surgical findings in 60 consecutive cases. *Surg Neurol* 53: 93-99, 2003
5. Furtado SV, Thakre DJ: Morphometric analysis of foramen magnum dimensions and intracranial volume in pediatric Chiari I malformation. *Acta Neurochir* 152: 221- 227, 2010
6. Hamlyn PJ: Neurovascular relationships in the posterior cranial fossa, with special reference to trigeminal neuralgia. 1. Review of the literature and development of a new method of vascular injection-filling in cadaveric controls. *Clin Anat* 10: 371- 379, 1997

7. Hamlyn PJ: Neurovascular relationships in the posterior cranial fossa, with special reference to trigeminal neuralgia. 2. Neurovascular compression of the trigeminal nerve in cadaveric controls and patients with trigeminal neuralgia: Quantification and influence of method. *Clin Anat* 10: 380-388, 1997
8. Lescanne E, Francois P, Velut S: Cerebellopontine cistern: Microanatomy applied to vestibular schwannomas. *Prog Neurol Surg* 21: 43-53, 2008
9. Lieberman DE, Pearson OM, Mowbray KM: Basicranial influence on overall cranial shape. *J Hum Evol* 38: 291-315, 2000
10. Lister JR, Rhoton AL Jr, Matsushima T, Peace DA: 618 Microsurgical anatomy of the posterior inferior cerebellar artery. *Neurosurgery* 10: 170-199, 1982
11. Mark PH, Yakovlev PI: A note on problems and methods in the preparation of a human stereotactic atlas; including a report of measurements of the posteromedial portion of the ventral nucleus of the thalamus. *Anat Rec* 121: 745-752, 1955
12. Matsushima T, Fukui M, Suzuki S, Rhoton AL Jr: The microsurgical anatomy of the infratentorial lateral supracerebellar approach to the trigeminal nerve for tic douloureux. *Neurosurgery* 24: 890-895, 1989
13. Mazzoni A: Internal auditory canal: Arterial relations at the porus acusticus. *Ann Otol Rhinol Laryngol* 78: 797-814, 1969
14. Murali R, Chandy MJ, Rajshekhar V: Neurovascular relationships of the root entry zone of lower cranial nerves: A microsurgical anatomic study in fresh cadavers. *Br J Neurosurg* 5: 349-356, 1991
15. Origitano TC, Anderson DE, Tarassoli Y, Reichman OH, al-Mefty O: Skull base approaches to complex cerebral aneurysms. *Surg Neurol* 40: 339-346, 1993
16. Pai BS, Varma RG, Kulkarni RN, Nirmala S, Manjunath LC, Rakshith S: Microsurgical anatomy of the posterior circulation. *Neurol India* 55: 31-41, 2010
17. Rhoton AL Jr: The cerebellar arteries. *Neurosurgery* 47(Suppl 3): S29-S68, 2000
18. Rusu MC, Ivascu RV, Cergan R: Typical and atypical neurovascular relations of the trigeminal nerve in cerebellopontine angle: An anatomical study. *Surg Radiol Anat* 31: 507-516, 2009
19. Saberi H, Kashfi A, Amidi F, Tabatabai SA: Correlation of cephalic anthropometric parameters and microsurgical anatomy of the optic nerves: A cadaveric morphometric study. *Surg Neurol* 60: 438-442, 2003
20. Sahin B, Acre N, Sonmez OF, Emirzeoglu M, Basaloglu H, Uzun A, Bilgic S: Comparison of four methods for the estimation of intracranial volume: A gold standard study. *Clin Anat* 20: 766-773, 2007
21. Sunderland S: The arterial relations of the internal auditory meatus. *Brain* 68: 23- 27, 1945
22. Surchev N: Arterial relationships to the nerves and some rigid structures in the posterior cranial fossa. *Clin Anat* 21: 492-500, 2008
23. Welsh LW, Welsh JJ, Jaffe SC, Healy MP: Evaluation of the vestibular system by magnetic resonance angiography. *Laryngoscope* 106: 1138-1143, 1996
24. Yasargil MG: Intracranial arteries. In: Yasargil MG, ed. *Microneurosurgery*. New York: Thieme Medical Publishers Inc, 1987: 54-168
25. Yurtseven T, Savaş R, Koçak A, Turhan T, Aktaş EO, İşlekel S: Relationship between anterior inferior cerebellar artery and facial-vestibulocochlear nerve complex: An anatomical and magnetic resonance images correlation study. *Minim Invasive Neurosurg* 47: 306-311, 2004